




Heterogenous expression of endoglin marks advanced renal cancer with distinct tumor microenvironment fitness

Yusaku Momoi¹ | Jun Nishida¹  | Kosuke Miyakuni¹ | Masafumi Kuroda² | Shimpei I. Kubota¹  | Kohei Miyazono¹  | Shogo Ehata^{1,3} 

¹Department of Molecular Pathology, Graduate School of Medicine, The University of Tokyo, Bunkyo-ku, Japan

²International Research Center for Neurointelligence (WPI-IRCIN), UTIAS, The University of Tokyo, Bunkyo-ku, Japan

³Environmental Science Center, The University of Tokyo, Bunkyo-ku, Japan

Correspondence

Shogo Ehata, Department of Molecular Pathology, Graduate School of Medicine, The University of Tokyo, 7-3-1 Hongo, 113-0033 Bunkyo-ku, Tokyo, Japan.
Email: ehata-jun@umin.ac.jp or shogoezata@g.ecc.u-tokyo.ac.jp

Funding information

Japan Society for the Promotion of Science (JSPS), (Grant/Award Number: 19K07684, 'KAKENHI Grant-in-Aid for Scientific Research (C)') the Ministry of Education, Culture, Sports, Science and Technology (MEXT) of Japan, (Grant/Award Number: 17H06326, 'KAKENHI Grant-in-Aid for Scientific Research on Innovative Area on Integrated Analysis and Regulation of Cellular Diversity') Princess Takamatsu Cancer Research Fund, (Grant/Award Number: 'none').

Abstract

Intratumoral heterogeneity, including in clear cell renal cell carcinoma, is a potential cause of drug resistance and metastatic cancer progression. We specified the heterogeneous population marked by endoglin (also known as CD105) in a preclinical model of clear cell renal cell carcinoma progression. Highly malignant derivatives of human clear cell renal cell carcinoma OS-RC-2 cells were established as OS5Ks by serial orthotopic inoculation in our previous study. Expression of both *ENG* (encoding endoglin) mRNA and protein were heterogeneously upregulated in OS5Ks, and the endoglin-positive (ENG^+) population exhibited growth dependency on endoglin in anchorage-independent cultures. Despite the function of endoglin as a type III receptor, transforming growth factor β and bone morphogenetic protein-9 signaling were unlikely to contribute to the proliferative phenotype. Although endoglin has been proposed as a marker for renal cancer-initiating cells, the OS5K-3 ENG^+ population did not enrich other reported cancer-initiating cell markers or differentiate into the ENG^- population. Mouse tumor inoculation models revealed that the tumor-forming capabilities of OS5K-3 ENG^+ and ENG^- cells in vivo were highly dependent on the microenvironment, with the renal microenvironment most preferable to ENG^+ cells. In conclusion, the renal microenvironment, rather than the hypothesized ENG^+ cell-centered hierarchy, maintains cellular heterogeneity in clear cell renal cell carcinoma. Therefore, the effect of the microenvironment should be considered when evaluating the proliferative capability of renal cancer cells in the experimental settings.

KEYWORDS

cancer stem cell, endoglin, renal cancer, tumor heterogeneity, tumor microenvironment

Abbreviations: 786-Pa, parental 786-O; ALK, activin receptor-like kinase; BMP, bone morphogenetic protein; ccRCC, clear cell renal cell carcinoma; CICs, cancer-initiating cells; CSCs, cancer stem cells; ENG, endoglin; GSK, glycogen synthase kinase; ID1, inhibitor of DNA binding 1; OSPa, parental OS-RC-2; PRAS40, proline-rich Akt1 substrate of 40 kDa; TGF- β , transforming growth factor β ; α -SMA, α -smooth muscle actin.

Momoi and Nishida these authors contributed equally to this work.

This is an open access article under the terms of the Creative Commons Attribution-NonCommercial-NoDerivs License, which permits use and distribution in any medium, provided the original work is properly cited, the use is non-commercial and no modifications or adaptations are made.

© 2021 The Authors. *Cancer Science* published by John Wiley & Sons Australia, Ltd on behalf of Japanese Cancer Association.

1 | INTRODUCTION

Renal cell carcinoma is the 13th most common cause of cancer-related deaths worldwide, with clear cell renal cell carcinoma (ccRCC) the most common histological type.^{1,2} Although the cure rate for early stage renal cancer is high, the prognosis of advanced disease with distant metastases is poor.² Cancer stem cell (CSC) or cancer-initiating cell (CIC) theories have been proposed to explain clinical difficulties, such as treatment resistance and metastasis. CSC/CIC was originally analyzed in hematopoietic cancer and some types of other solid cancers, in which mutations in stem cells or early progenitors might give rise to the development of cancer. Therefore, the initial CSC/CIC theory supports a hierarchical model that argues for the existence of a particular population of cells characterized by self-renewal, high tumorigenicity, and the capability to reconstitute the cellular heterogeneity. Subsequent studies have also shown that cancer cells exhibit plasticity or activate the transcriptional program of their ancestors or distinct lineages, resulting in the production of CICs.³⁻⁵ In this setting, it is still controversial whether all the cancer cell populations in the tumor are explained in the hierarchical model, implying the difficulty of targeted therapy against a particular population. Several molecules normally expressed in specific cell lineages have been proposed as the CSC/CIC markers in many types of cancer, including in renal cancer.^{6,7}

The interaction between cancer cells and the tumor microenvironment is essential for the acquisition of malignant phenotypes and the maintenance of CSC/CICs.⁴ We have identified the molecular mechanisms underlying tumor progression by applying orthotopic tumor inoculation models to simulate the interaction with the tumor microenvironment.⁸⁻¹² As for ccRCC, we focused on the roles of transforming growth factor β (TGF- β) family signaling, including TGF- β and BMP, as mediators of the interaction. TGF- β family signaling involves 2 types of kinase receptors: type I and type II. Upon ligand binding, type I and II receptors form a complex to transduce signals by the activation of Smad proteins, as well as by non-Smad pathways, such as the MAPK pathways.^{13,14} We previously reported that high expression of c-Ski, a transcriptional co-repressor, accelerated the progression of ccRCC by attenuating Smad-dependent TGF- β signaling.¹⁰ TGF- β family signaling is also modified by co-receptors called type III receptors, which include betaglycan (TGFB3) and endoglin (ENG, also known as CD105).¹³ In our previous study, low betaglycan expression in ccRCC cells contributed to their metastatic capabilities by enhancing cellular migration, as well as by the attenuation of TGF- β 2-mediated decrease of aldehyde dehydrogenase (ALDH)-positive cancer cells, in which CICs were enriched.⁸ Endoglin is preferentially characterized in endothelial cells as well as mesenchymal stem cells.¹⁵ Endoglin on vascular endothelial cells is regarded as a target for ccRCC therapy as exemplified by the clinical development of Carotuximab (TRC105).^{16,17} Renal cancer cells have also been reported to express endoglin. The expression of endoglin in cancer cells, rather than that in endothelial cells, correlates with poor prognosis in ccRCC patients.¹⁸ Notably, endoglin has been reported to be heterogeneously expressed and enriched

CIC population of renal cancer.^{6,7,19,20} However, the dynamics of endoglin-expressing ccRCC cells during tumor progression have not been well characterized.

The present study aimed to investigate the impact of endoglin expression in ccRCC progression. Toward this goal, we examined the CSC/CIC properties of endoglin-positive (ENG⁺) ccRCC cells and their tumor-forming capabilities in various microenvironments.

2 | MATERIALS AND METHODS

2.1 | Cell culture

Human ccRCC cells OS-RC-2 (RIKEN Cell Bank) and their derivatives were cultured in RPMI 1640 medium (Thermo Fisher Scientific) containing 10% fetal bovine serum (FBS), unless otherwise described. The establishment of OS-RC-2 derivatives stably expressing mCherry has been described previously.⁹

2.2 | Renal orthotopic tumor model

All animal experiments were approved by the Animal Ethics Committee of The University of Tokyo. OS-RC-2 derivatives were suspended in 50 μ l HBSS and inoculated into the renal subcapsule of BALB/*c-nu/nu* mice (5-wk-old males) as previously described.^{9,21} Tumor weights were calculated by subtracting the weight of the unaffected kidney from that of the tumor-bearing kidney for each sample.

2.3 | Evaluation of metastasis using tissue clearing

For the detection of metastatic tumors in mouse models, the whole brain and lung were cleared by CUBIC-L/R as previously described.^{21,22} The brains of the mice were co-stained with anti- α -smooth muscle actin (α -SMA) antibody, as indicated in Table S1. Images were acquired with a light-sheet fluorescence microscopy RAPID with a $\times 0.63$ objective. Metastatic tumors were evaluated based on mCherry expression visualized using ImageJ software (National Institutes of Health, MD, USA). Computational methods for the quantification of metastasis have been described previously.²³

2.4 | Statistical analysis

Comparisons between 2 independent samples were performed using a two-sided Student *t* test or Welch *t* test, depending on the results of the *F*-test. Comparisons between 2 paired groups and among groups were performed using a paired *t* test and using one-way ANOVA followed by Tukey multiple comparison test. All statistical analyses were performed using Prism 6 software (GraphPad).

Significant differences were defined as $*P < .05$, $**P < .01$, and $***P < .001$.

2.5 | Other methods

Further information on material and method is provided in Supporting Information (Table S2, S3, Appendix S1).

3 | RESULTS

3.1 | Characterization of the proliferative phenotype of ENG^+ ccRCC cells

In our previous study,⁹ we utilized serial orthotopic inoculation of human ccRCC cells (parental OS-RC-2 [OSP_a] or parental 786-O [786-Pa]) and established highly malignant derivatives, namely, OS5K-1, OS5K-2, and OS5K-3, or 786-3K. In this study, RNA-sequencing analysis in our published data revealed that *ENG* mRNA expression was higher in the derivatives compared with that in OSP_a cells (Figure 1A). Furthermore, chromatin immunoprecipitation (ChIP)-sequencing analysis for the acetylation of histone H3 at lysine-27 (H3K27ac) showed that the H3K27ac levels near the transcription start site of *ENG* gene locus were higher in the derivatives compared with those in OSP_a cells (Figure 1B). Endoglin protein expression exhibited the same trend as *ENG* mRNA expression (Figure 1C). Moreover, flow cytometric analysis revealed that the ENG^+ population was higher in the derivatives compared with that in the parental cells (Figures 1D and S1A). ENG^+ cells comprised more than 50% of the cell population in OS5K-2 and OS5K-3 and approximately 15% in OSP_a (Figure 1D). An analysis of clinical data also showed that *ENG* mRNA expression was upregulated in ccRCC tissues compared with that in adjacent normal tissues (Figure S1B). Therefore, to characterize the increased population of ENG^+ cells in OS5K-3, ENG^+ and ENG^- cells were sorted from OSP_a and OS5K-3 cells (Figure S1C). Quantitative real-time PCR (qRT-PCR) analysis showed that *ENG* mRNA expression was upregulated in OS5K-3 ENG^+ cells compared with that in OSP_a ENG^+ cells (Figure 1E). To analyze the proliferative and colony-forming capability of OS5K-3 ENG^+ cells, we used a cell proliferation assay in 2D culture and agar gel-based colony formation assay in 3D culture. These assays showed that OS5K-3 ENG^+ cells exhibited significantly faster proliferation (Figure 1F) and anchorage-independent growth (Figure 1G) compared with OS5K-3 ENG^- cells and OSP_a cells. These results suggested that endoglin expression was modified by exposure to the renal microenvironment, which may account for the phenotype of rapid proliferation.

To investigate whether endoglin upregulation is sufficient to promote rapid proliferation, we next established OSP_a cells expressing *ENG* (Figure 2A,B). *ENG* overexpression slightly, but significantly, promoted the proliferation rate of OSP_a cells (Figure 2C). Next, to investigate whether endoglin is essential for anchorage-independent growth of OS5K-3 ENG^+ cells, we knocked down the

expression of *ENG* gene either by short hairpin RNAs (shRNAs) or by small interfering RNAs (siRNAs) (Figure 2D, Figure S2A). Endoglin knockdown by shRNAs attenuated the anchorage-independent growth of OS5K-3 ENG^+ cells in vitro (Figure 2E). A similar result was obtained in siRNA-mediated silencing of endoglin (Figure S2B). The introduction of shRNA also attenuated anchorage-independent growth of unsorted OS5K-3 cells (Figure 2F,G). These results suggested that the growth of OS5K-3 ENG^+ cells is dependent on endoglin in anchorage-independent cultures. However, upregulation of endoglin by itself does not fully promote the tumor cell proliferation observed in OS5K-3 ENG^+ cells, implying the existence of unknown cofactors that cooperate with endoglin to stimulate cell division.

3.2 | Identification of the signaling pathway activated in ENG^+ renal cancer cells

To investigate the mechanism by which endoglin promotes the proliferation of OS5K-3 ENG^+ cells, we first focused on the function of endoglin as a type III TGF- β receptor. Endoglin modulates TGF- β family signaling in endothelial cells, especially by upregulation of activin receptor-like kinase (ALK)1-Smad1/5/8 signaling and downregulation of TGF- β -ALK5-Smad2/3 signaling.¹³ Therefore, we hypothesized that endoglin attenuates TGF- β -induced growth inhibition in ENG^+ ccRCC cells by attenuating phosphorylation of Smad2/3. Although TGF- β induced the phosphorylation of both Smad2 and Smad1/5/8, there was no significant difference between OS5K-3 ENG^+ and ENG^- cells (Figure 3A,B). shRNA-mediated knockdown of *ENG* enhanced TGF- β 1-induced phosphorylation of Smad2, suggesting that endoglin functionally attenuates TGF- β -ALK5-Smad2/3 signaling in OS5K-3 ENG^+ cells (Figure 3C). In contrast, TGF- β 1, 2, and 3 significantly suppressed the anchorage-independent growth of OS5K-3 ENG^+ cells to different extents (Figure 3D). These results suggested a limited contribution of TGF- β signaling to the highly proliferative phenotype of OS5K-3 ENG^+ cells.

Endoglin acts as an accessory receptor that forms complexes with ALK1 and enhances BMP-9-ALK1-Smad1/5 signaling in endothelial cells.²⁴ We therefore hypothesized that enhanced sensitivity to BMP-9 promotes the proliferation of OS5K-3 ENG^+ cells and accordingly investigated the roles of BMP-9-ALK1-Smad1/5/8 signaling in OS5K-3 ENG^+ cells. A preliminary experiment verified that FBS increased Smad1/5/8 phosphorylation in a dose-dependent manner (Figure 4A). This was canceled by LDN193189, a small-molecule ALK1/2/3/6 inhibitor, indicating the presence of BMPs in FBS (Figure 4B). Therefore, we reduced FBS concentration and investigated the effects of exogenous BMP-9 on renal cancer cells. Phosphorylation of Smad1/5/8 and the expression of its target gene, inhibitor of DNA binding 1 (*ID1*), were induced by the stimulation with BMP-9. This was in turn attenuated by the knockdown of endoglin, suggesting that endoglin functionally participates in BMP-9-Smad1/5/8 signaling in OS5K-3 ENG^+ cells (Figure 4C,D). However, phosphorylation of Smad1/5/8 was not enhanced in OS5K-3 ENG^+ cells compared with ENG^- cells across all FBS concentrations with or

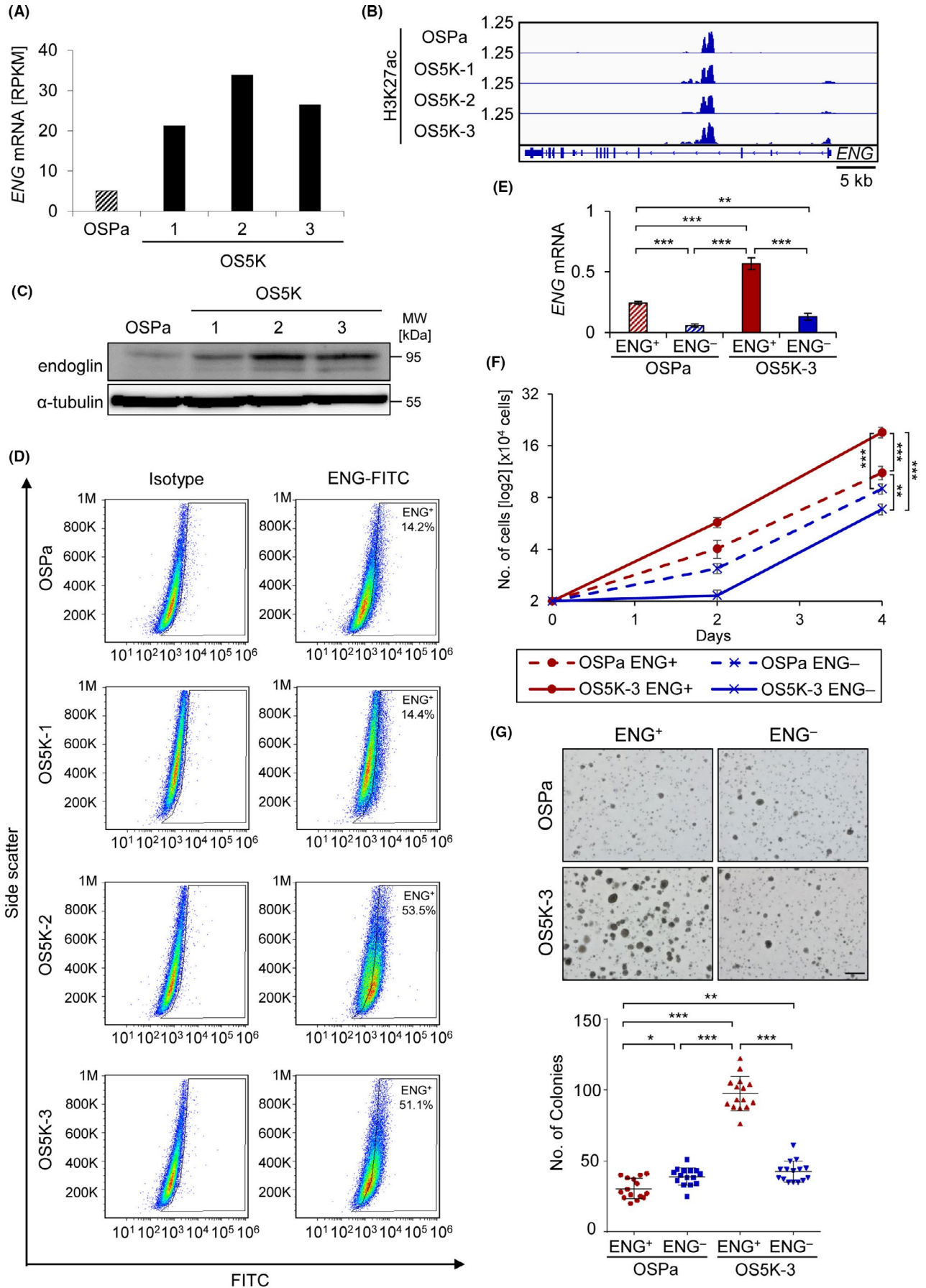


FIGURE 1 Endoglin-positive population in highly malignant ccRCC cells has a characteristic of rapid proliferation in vitro. A, *ENG* mRNA expression in RNA-sequencing analysis of OS-RC-2 derivatives (re-analyses of the data in GSE131137). B, H3K27ac peaks near the *ENG* gene region in OS-RC-2 derivatives (re-analyses of the data in GSE131139). C, Immunoblots for the indicated proteins of OS-RC-2 derivatives. D, Percentage of ENG^+ population in OS-RC-2 derivatives (flow cytometry). E, *ENG* mRNA expression of sorted OSPa and OS5K-3 ENG^+ and ENG^- cells (qRT-PCR; Tukey multiple comparison test). F, Cell proliferation assay for sorted OSPa and OS5K-3 ENG^+ and ENG^- cells in 2D culture (Tukey multiple comparison test). G, Colony formation assay for sorted OSPa and OS5K-3 ENG^+ and ENG^- cells. Top panel: Images of colonies; bottom panel: numbers of colonies counted on day 18 (Tukey multiple comparison test; scale bar, 500 μ m). All data are presented as the mean \pm SD. * $P < .05$, ** $P < .01$, *** $P < .001$. MW, molecular weight

without BMP-9 (Figure 4A). Functionally, BMP-9 slightly decreased the colony formation of OS5K-3 ENG^+ cells, contrary to the hypothesis of BMP-9-induced proliferation (Figure 4E). Of note, qRT-PCR analysis showed that the expression of *ACVRL1* (encoding ALK1) was significantly higher in OS5K-3 ENG^- cells compared with that in ENG^+ cells (Figure 4F). This might be responsible for the similar phosphorylation levels of Smad1/5/8 between OS5K-3 ENG^+ and ENG^- cells. Overall, these results suggested that neither TGF- β nor BMP-9 signaling explains the highly proliferative phenotype of OS5K-3 ENG^+ cells in vitro.

Therefore, we then attempted to identify the signaling pathways involved in the proliferation of OS5K-3 ENG^+ cells. Phospho-kinase array analysis revealed differences in phosphorylation profiles between ENG^+ and ENG^- cells in OSPa and OS5K-3 (Figure 5A). In particular, the phosphorylation levels of Akt (T308), proline-rich Akt1 substrate of 40 kDa (PRAS40) (T246), and glycogen synthase kinase (GSK)-3 α/β (S21/S9) were upregulated in OS5K-3 ENG^+ cells compared with those in OSPa cells and OS5K-3 ENG^- cells. PRAS40²⁵ and GSK-3 α/β ²⁶ are known to be downstream proteins of Akt signaling. Akt phosphorylation (T308) in OS5K-3 ENG^+ cells was confirmed by immunoblotting of independent lysates of OS5K-3 ENG^+ and ENG^- cells (Figure 5B). However, knockdown of *ENG* did not strongly alter the phosphorylation levels of Akt, although a slight reduction was observed (Figure 5C, Figure S3). These results suggested that Akt signaling is upregulated in OS5K-3 ENG^+ cells in vitro, but endoglin might have limited effect on the pathway.

3.3 | Assessment of the cancer stem cell-like potential of ENG^+ cells

We next validated the CSC/CIC properties of OS5K-3 ENG^+ cells because endoglin has been reported to be a marker for cancer stem-like cells in renal cell carcinoma.^{6,7,19,20} Therefore, we first examined the expression of markers reported to be enriched in CSC/CICs, including *CD44*, *CD24*, *CXCR4*, *ALDH1A1*, *POU5F1* (encoding Oct4), *MYC*, *KLF4*, and *PROM1* (encoding CD133).^{6,7,27,28} However, their expression was not necessarily high in ENG^+ cells sorted from OS5K-3 or 786-3K cells compared with that in ENG^- cells (Figure 6A, Figure S4A). Based on CSC theory, stem-like cells can reconstitute the “differentiated” population of cancer cells by asymmetric cell division. Therefore, we examined whether OS5K-3 ENG^+ cells re-established both ENG^+ and ENG^- cells in a long-term culture. However, the sorted ENG^+ cell population remained homogeneous with high expression of endoglin, implying that ENG^+ cells did not reproduce ENG^- cells, and

vice versa (Figure 6B, Figure S4B). We also investigated whether CICs were enriched in OS5K-3 ENG^+ cells using an orthotopic inoculation model. ENG^+ cells did not exhibit increased tumor-forming capability compared with ENG^- cells, even with fewer numbers of inoculated cells (Figure 6C-F). Although endoglin is important for the highly proliferative phenotype and anchorage-independent growth of renal cancer cells, endoglin-expressing cells do not serve as renal cancer stem-like cells, at least in our model.

3.4 | Evaluation of the tumor-forming and metastatic capabilities of ENG^+ cells in various tumor microenvironments

Although OS5K-3 ENG^+ cells showed increased anchorage-independent growth in vitro (Figure 1G), their tumor-forming capability was not different from that of ENG^- cells in the orthotopic inoculation model in vivo (Figure 6C-F). This discrepancy led us to hypothesize that the tumor microenvironment determines the proliferative capability of ccRCC cells. Therefore, tumor-forming capabilities were examined in the subcutaneous environment as well as the environments in common metastatic sites for renal cancer, using several mouse tumor models. In the subcutaneous inoculation model, OS5K-3 ENG^- cells exhibited significantly increased tumor-forming capability compared with ENG^+ cells (Figure 7A). In the intravenous injection of tumor cells, OS5K-3 ENG^- cells formed more experimental metastatic lung tumors compared with ENG^+ cells (Figure 7B). In contrast, in the intracardiac injection of tumor cells, OS5K-3 ENG^+ and ENG^- cells formed similar levels of metastatic brain tumors (Figure 7C). Overall, these results suggested that the tumor-forming and metastatic capabilities of ENG^+ and ENG^- cells are highly dependent on their microenvironment.

4 | DISCUSSION

The present study examined the role of endoglin in the progression of ccRCC both in vitro and in vivo. ENG^+ cells, the proportion of which is thought to be increased in the interaction with their renal microenvironments, exhibited an endoglin-dependent highly proliferative phenotype in vitro. However, ENG^+ cells did not necessarily act as CSC/CICs, and ENG^+ and ENG^- cells showed distinct tumorigenic characteristics under several different microenvironments in vivo.

Endoglin has been proposed as a marker for renal cancer stem-like cells or CICs, although this remains controversial. This was first

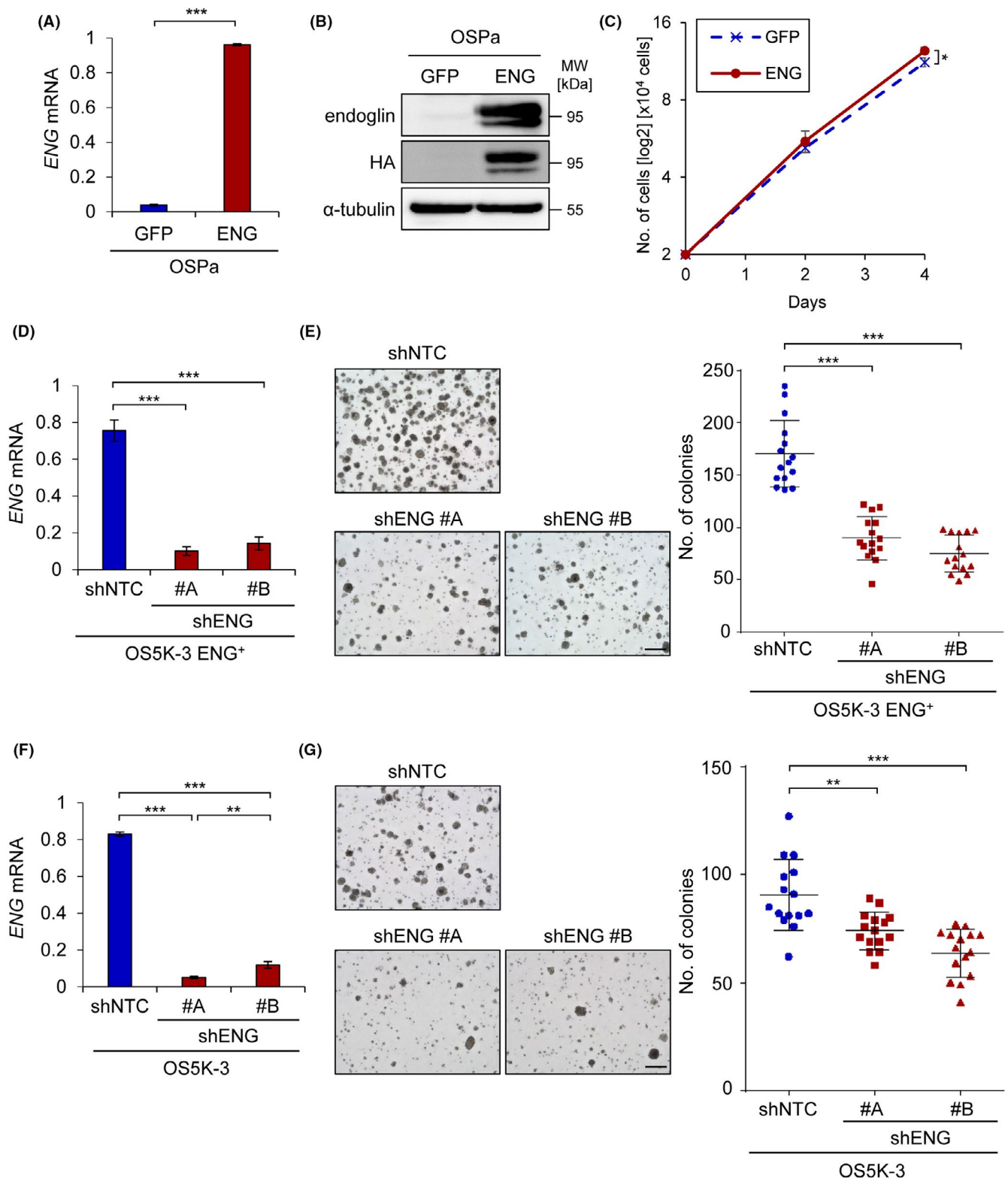


FIGURE 2 Endoglin is essential for the anchorage-independent growth of ENG⁺ ccRCC cells in vitro. A, ENG mRNA expression of GFP- or hemagglutinin (HA)-tagged endoglin-overexpressing OSPA cells (qRT-PCR; Welch *t* test). B, Immunoblots for the indicated proteins of GFP- or HA-tagged endoglin-overexpressing OSPA cells. C, Cell proliferation rates of GFP- or ENG-expressing OSPA cells in 2D culture (Student *t* test). D, ENG mRNA expression of shRNA-introduced OS5K-3 ENG⁺ cells (qRT-PCR; Tukey multiple comparison test). E, Colony formation assay for shRNA-introduced OS5K-3 ENG⁺ cells. Left panels: Representative images. Right panel: numbers of colonies counted on day 18 (Tukey multiple comparison test; scale bar, 500 μ m). F, ENG mRNA expression of shRNA-introduced OS5K-3 cells (qRT-PCR; Tukey multiple comparison test). G, Colony formation assays for shRNA-introduced OS5K-3 cells. Left panel: representative images; right panel: numbers of colonies counted on day 19 (Tukey multiple comparison test; scale bar, 500 μ m). All data are presented as the mean \pm SD. **P* < .05, ***P* < .01, ****P* < .001

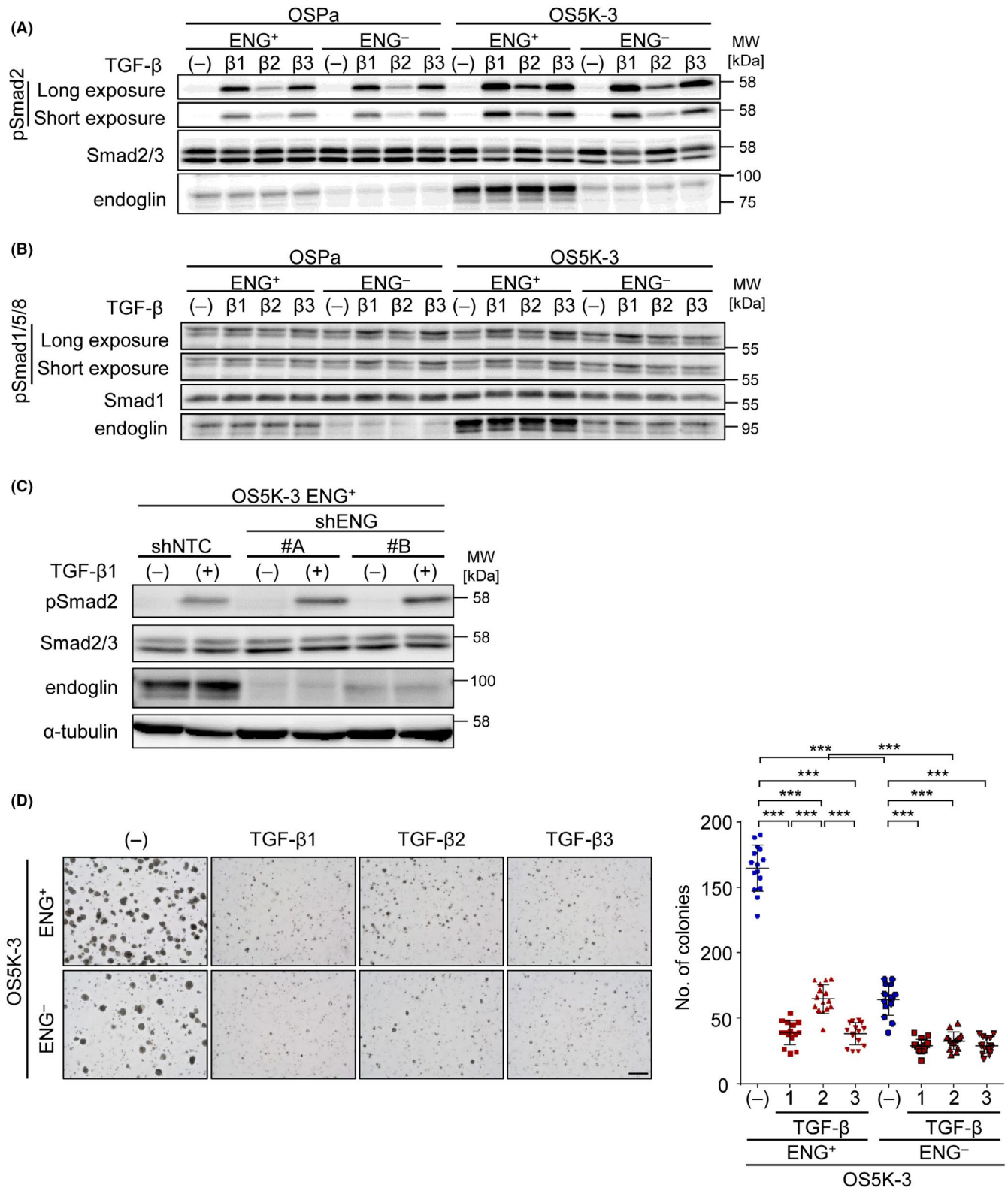


FIGURE 3 Transforming growth factor β provides only a limited explanation for the function of endoglin in ENG⁺ ccRCC cells. A, Immunoblots of cell lysates with the indicated antibodies. OSPα and OS5K-3 ENG⁺ and ENG⁻ cells were treated with TGF- β for 1 h (β 1, TGF- β 1; β 2, TGF- β 2; β 3, TGF- β 3). B, Immunoblots of cell lysates with the indicated antibodies. OSPα and OS5K-3 ENG⁺ and ENG⁻ cells were pre-cultured under 1% FBS for 1 d and treated with TGF- β for 1 h (β 1, TGF- β 1; β 2, TGF- β 2; β 3, TGF- β 3). C, Immunoblots of cell lysates with the indicated antibodies. shRNA-transfected OS5K-3 ENG⁺ cells were treated with TGF- β 1 for 1 h. D, Colony formation assay for TGF- β -stimulated OS5K-3 ENG⁺ and ENG⁻ cells. Left panel: representative images; right panel: number of colonies counted on day 21. Data are presented as the mean \pm SD (Tukey multiple comparison test; scale bar, 500 μ m). *** P < .001

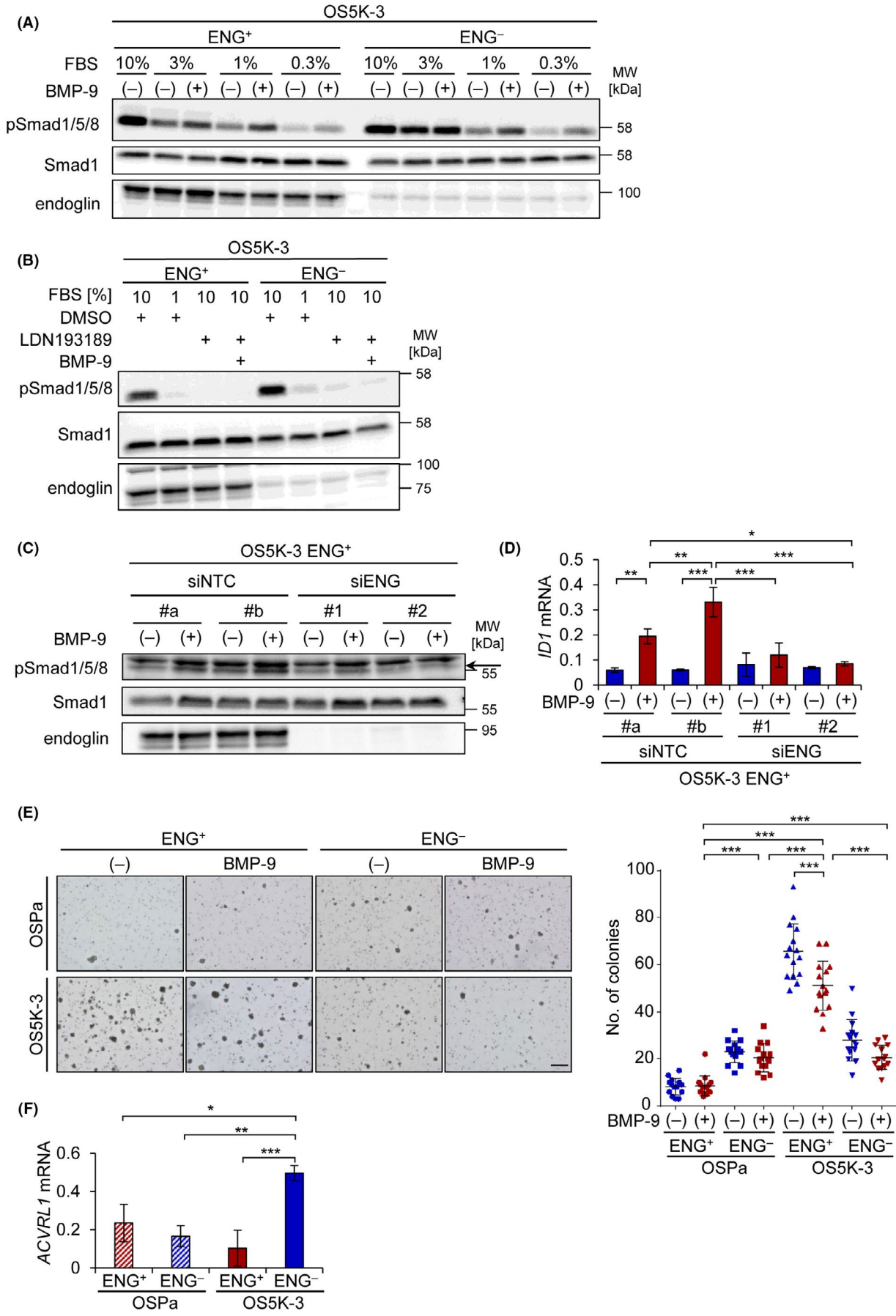


FIGURE 4 Bone morphogenetic protein-9 does not explain the function of endoglin in ENG^+ ccRCC cells. A, Immunoblots of cell lysates with the indicated antibodies. Cells were pre-cultured with the indicated FBS concentration for 1 d and treated with BMP-9 for 1 h. B, Immunoblots of cell lysates with the indicated antibodies. Cells were pre-treated with 0.1 $\mu\text{mol/L}$ LDN193189 or DMSO for 1 d under the indicated FBS concentration and then stimulated with BMP-9 for 1 h. C, Immunoblots of cell lysates with the indicated antibodies. OS5K-3 ENG^+ cells were cultured under 1% FBS and subsequently transfected with siRNA. After 3 d, cells were stimulated with BMP-9 for 1 h. D, *ID1* mRNA expression of siRNA-introduced and BMP-9-stimulated OS5K-3 ENG^+ cells (qRT-PCR). Cells were pre-cultured under 1% FBS for 1 d prior to siRNA transduction. After 3 d, cells were stimulated with BMP-9 for 2 h (Tukey multiple comparison test). E, Colony formation assay for BMP-9-stimulated OSPa and OS5K-3 ENG^+ and ENG^- cells cultured in 3% FBS. Left panel: representative images; right panel: number of colonies counted on day 19 (Tukey multiple comparison test; scale bar, 500 μm). F, *ACVRL1* mRNA expression of sorted OSPa and OS5K-3 ENG^+ and ENG^- cells (qRT-PCR; Tukey multiple comparison test). All data are presented as the mean \pm SD. * $P < .05$, ** $P < .01$, *** $P < .001$

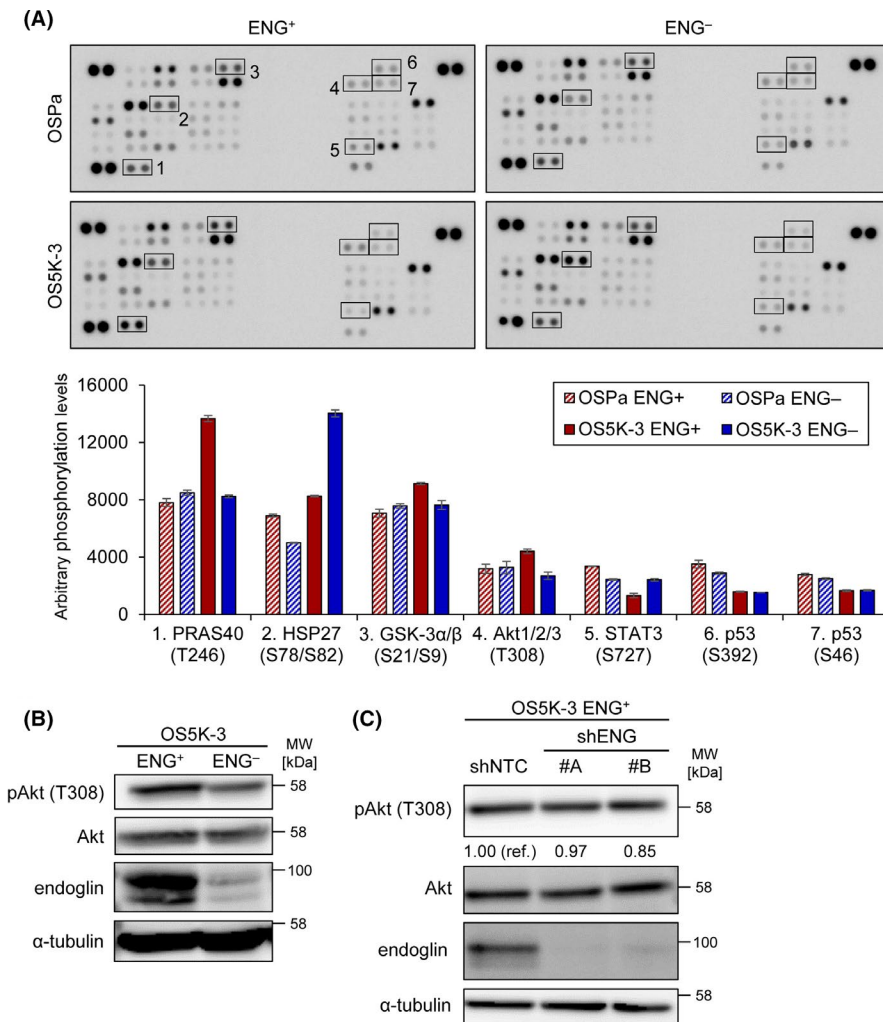


FIGURE 5 Akt signaling is upregulated in ENG^+ tumor cells. A, Phospho-kinase array of OS-RC-2 derivatives. Top panel: immunoblotted membranes (highlighted squares: spots with obvious differences in phosphorylation levels); bottom panel: quantifications of phosphorylation levels of the highlighted spots (bars: mean \pm SD of technical duplicate). B, Immunoblots for the indicated proteins of sorted OS5K-3 ENG^+ and ENG^- cells. C, Immunoblots for the indicated proteins of shRNA-introduced OS5K-3 ENG^+ cells (numbers: signal ratio of pAkt/Akt compared with that of shNCT)

reported using patient-derived ccRCC or undifferentiated renal cancer cells, in which CICs were defined as cells with the following properties: clonogenic capability; the potential to differentiate both in vitro and in vivo; and enhanced expression of the markers for stemness, including Oct4.¹⁹ Later, it was shown that ENG^+ cells formed more colonies in vitro than did ENG^- cells and expressed mesenchymal stem cell markers, including CD44, in ACHN and Caki-2 cells.²⁹ In addition, endoglin has been reported to be essential for tumor formation, gemcitabine resistance, and epithelial-mesenchymal transition (EMT) phenotype in the papillary renal cell carcinoma cells ACHN.^{20,30}

However, a recent study that used the Caki-1 cells derived from skin metastasis of ccRCC indicated that CD44⁺/ ENG^- cells enriched CSCs.³¹ In this study, CSCs had high tumorigenicity with distinctive angiogenic and metabolic characteristics in subcutaneous models. Therefore, we examined the tumorigenicity in several microenvironments, including in the kidney, and verified whether endoglin serves as a marker for CSC/CICs in ccRCC, using parental ccRCC cells OS-RC-2 and their derivatives. In an in vivo orthotopic tumor model, ENG^+ cells did not exhibit higher tumorigenicity than ENG^- cells. In contrast, ENG^- cells showed higher tumorigenicity under some experimental conditions, such as in the subcutaneous inoculation

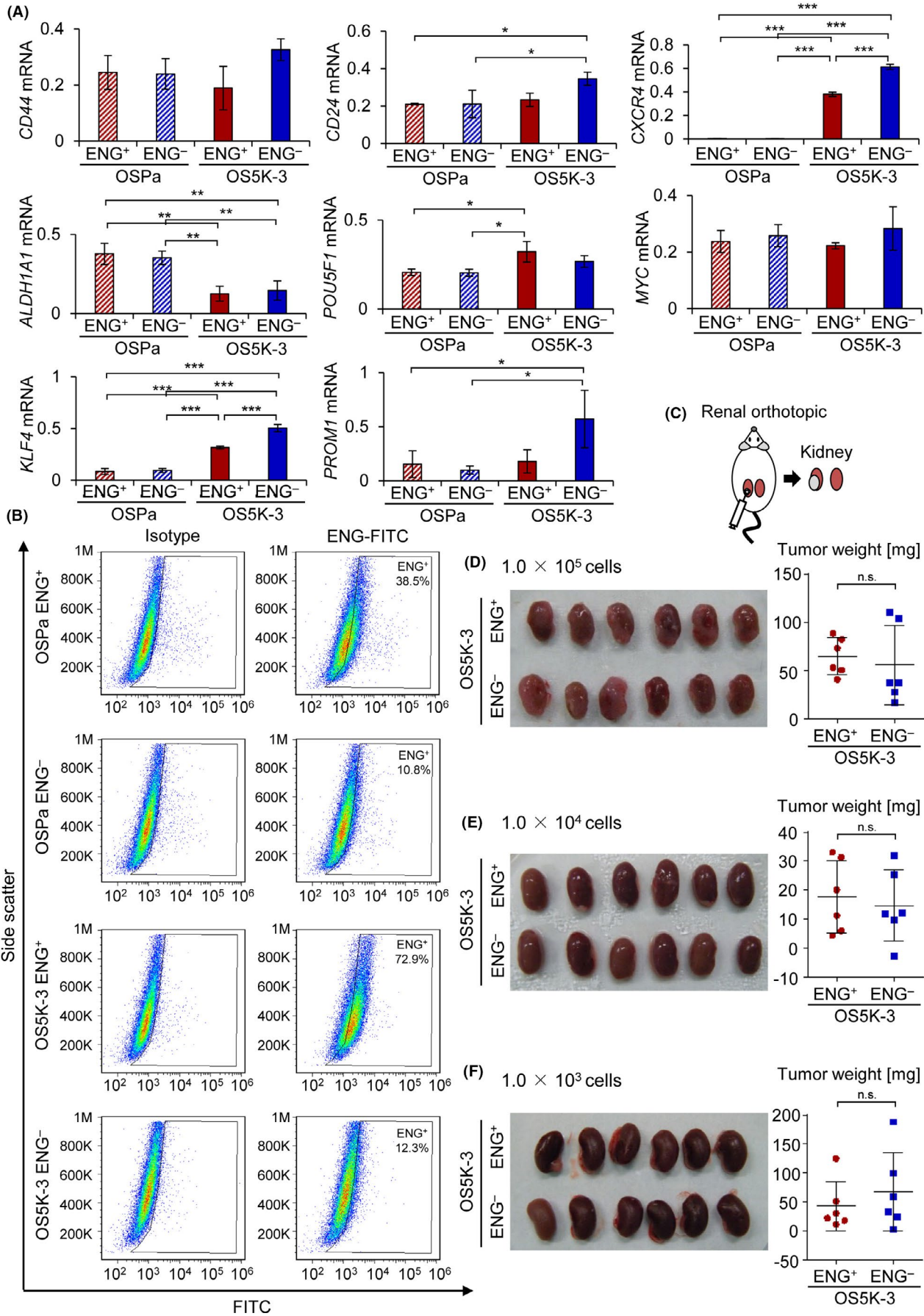


FIGURE 6 Endoglin-positive cells do not exhibit cancer stem cell-like traits. A, mRNA expression of the indicated genes in sorted OSPa and OS5K-3 ENG⁺ and ENG⁻ cells (qRT-PCR; Tukey multiple comparison test). B, Endoglin expression in OSPa and OS5K-3 ENG⁺ and ENG⁻ cells cultured for 16 d after the sorting (flow cytometry). C-F, Orthotopic inoculation model of sorted OS5K-3 cells. C, Schematic overview. D-F, Tumor-forming capability of OS5K-3 ENG⁺ or ENG⁻ cells. Cells (D, 1.0×10^5 cells, E, 1.0×10^4 cells, F, 1.0×10^3 cells/mice) were inoculated into the kidney orthotopically. The mice were sacrificed 18 d (D, E) or 71 d (F) after the inoculation. Left panel: tumor-bearing kidneys; right panel: tumor weights (n = 6/group; Student t test). All data are presented as the mean \pm SD. * $P < .05$, ** $P < .01$, *** $P < .001$; n.s., not significant

model. In addition, ENG⁺ cells did not reproduce ENG⁻ cells in long-term cultures. These results did not support the simplified ENG⁺ cell-centered CSC theory. They alternatively suggested that ENG⁺ and ENG⁻ cells may be distinct lineages and may have different characteristics. Each lineage may have a distinct spectrum of tumor-forming capability under various primary and metastatic microenvironments, a distinct signaling profile, and a distinct spectrum of drug sensitivity. Therefore, the therapeutic strategy for ccRCC may need to be a cellular heterogeneity- or microenvironment-oriented approach rather than being CSC/CIC-oriented. In this study, we could not clarify the mechanism by which endoglin expression is upregulated. The origin of ENG⁺ cells and whether cells highly expressing endoglin are from a unique lineage throughout ccRCC progression should be addressed in future studies.

We previously found that TGF- β -mediated tumor suppression is attenuated in ccRCC^{8,10}; therefore, we hypothesized that endoglin, a type III TGF- β receptor, also has a pro-proliferative role by modulating TGF- β family signaling. However, neither TGF- β nor BMP-9 signaling largely contributed to the difference in proliferative activity between OS5K-3 ENG⁺ and ENG⁻ cells (Figures 3 and 4). Therefore, we explored other signaling pathways that might promote the survival and proliferation of ENG⁺ cells. Based on the results of phospho-kinase array analysis (Figure 5A), we hypothesized that endoglin promoted the proliferation of ENG⁺ cells by activating the Akt pathway. Indeed, a phosphatidylinositol 3-kinase (PI3K) inhibitor and mechanistic target of rapamycin (mTOR) inhibitor effectively suppressed anchorage-independent proliferation of ENG⁺ cells (data not shown). A previous study using vascular endothelial cells, in which endoglin was preferentially expressed, also reported that the intracellular domain of endoglin activated PI3K and Akt signaling through an adaptor protein named G α -interacting protein C-terminus-interacting protein (GIPC).³² However, in the present study, knockdown of endoglin did not significantly alter the phosphorylation level of Akt, suggesting that it had limited influence on the Akt pathway. Another possibility is that the signaling pathways crucial for ENG⁺ cells are masked by the crosstalk of signaling. Differences in the expression of several genes (Figure 6A) and the microenvironment-dependent tumorigenicity (Figure 7) may suggest that the ENG⁺ and ENG⁻ cells have distinct characteristics and therefore cannot be simply compared in one signaling pathway. Previous studies have suggested other possible mechanisms by which endoglin promotes cancer cell proliferation. One study on pancreatic cancer cells found that inhibition of the interaction between endoglin and GIPC attenuated cell proliferation, induced cell differentiation, and sensitized the cells to gemcitabine.³³ Therefore, the intracellular domain of endoglin

may be involved in the promotion of ccRCC cell proliferation by interacting with other molecules, whether it be involved in Akt signaling or not.

The present study also showed the importance of the tumor microenvironment in cancer cell proliferation. ENG⁺ cells showed a superior proliferative capability to ENG⁻ cells in vitro (Figure 1F,G). However, their tumor-forming capability in vivo was similar to that of ENG⁻ cells in the orthotopic inoculation model (Figure 6C-F) and experimental brain metastasis model (Figure 7C), and inferior in the subcutaneous inoculation model (Figure 7A) and experimental lung metastasis model (Figure 7B). This suggests that there are different mechanisms of tumor formation in the various tumor microenvironments, and these differences can be mainly attributed to the differences in extracellular matrices, humoral factors, or other unknown factors. In particular, ENG⁺ cells exhibited the most enhanced tumorigenicity in their primary site of the kidney, indicating that the primary tumor microenvironment plays an important role in maintaining cellular heterogeneity. Notably, endoglin plays a critical role in angiogenesis and is one of the genes responsible for hereditary hemorrhagic telangiectasia (Osler-Weber-Rendu disease).³⁴ A previous study reported that ENG⁻/CD44⁻ renal cancer cells displayed a distinctive capability to induce angiogenesis.³¹ The interference of endothelial signaling may have resulted in the failure in angiogenesis and the lower tumorigenic capability of ENG⁺ cells in subcutaneous inoculation model compared with colony formation in vitro, in which angiogenesis is not needed.

In conclusion, these results support that the renal microenvironment, rather than the hypothesized ENG⁺ cell-centered hierarchy, maintains cellular heterogeneity in ccRCC. Therefore, the effect of the microenvironment should be considered when evaluating the proliferative capability of renal cancer cells in the experimental settings.

ACKNOWLEDGMENTS

We thank K. Takahashi (The University of Tokyo) for her technical assistance. We also thank H. Miyoshi (deceased, formerly Keio University) for providing the lentiviral vectors and P. ten Dijke (Leiden University) for providing the cloned plasmid of HA-tagged ENG. We also thank the support of the IRCN Imaging Core, The University of Tokyo Institutes for Advanced Studies. We also thank the Medical Scientist Training Program, Faculty of Medicine, The University of Tokyo for educational support (to YM). This work was supported by a KAKENHI Grant-in-Aid for Scientific Research on Innovative Area on Integrated Analysis and Regulation of Cellular Diversity from the Ministry of Education,

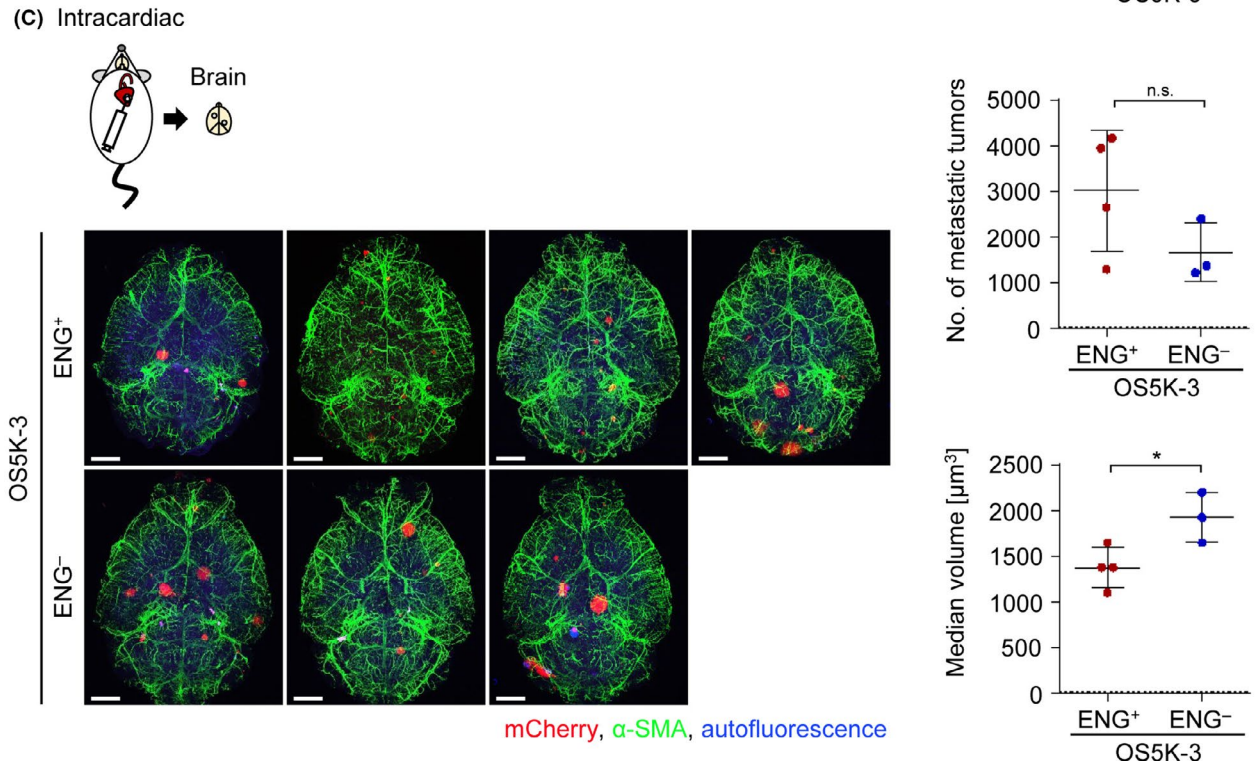
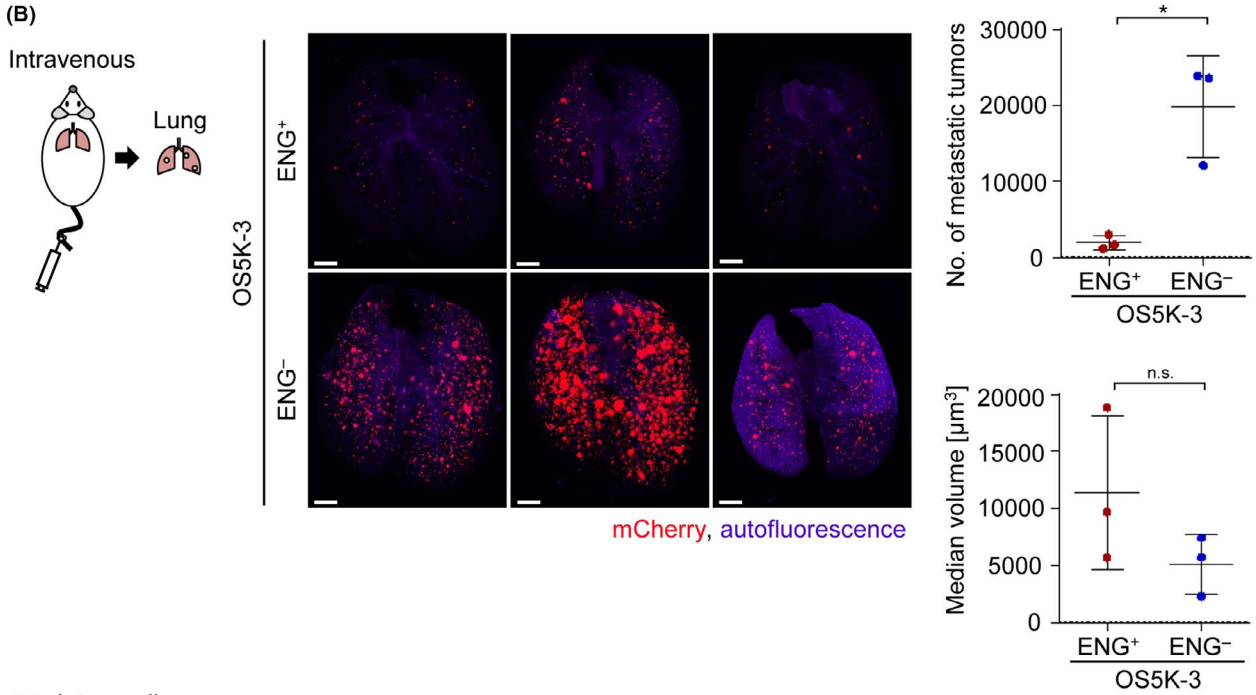
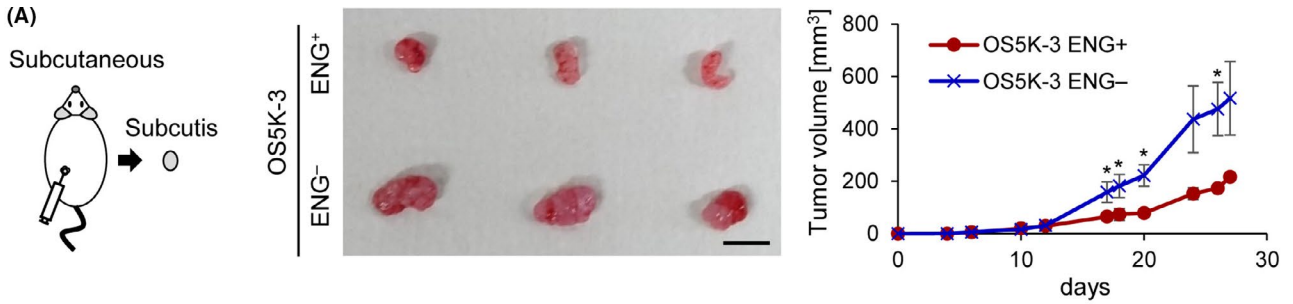


FIGURE 7 Tumor-forming and metastatic capabilities of ENG^+ and ENG^- cells are dependent on their microenvironments. A, Subcutaneous tumor-forming capability of OS5K-3 ENG^+ or ENG^- cells. Left panel: schematic overview; middle panel: image of the tumors excised 27 d after the inoculation; right panel: tumor volumes on the indicated days ($n = 3/\text{group}$; Welch t test; scale bars, 1 cm). B, Metastatic lung tumor-forming capability of OS5K-3 ENG^+ or ENG^- cells. Left panel: schematic overview; middle panel: images; right panel: numbers and median volumes of tumors ($n = 3/\text{group}$; Welch t test for the numbers and Student t test for the median volumes; scale bar, 2 mm). C, Metastatic brain tumor-forming capability of OS5K-3 ENG^+ or ENG^- cells. Top left panel: schematic overview; bottom left panel: images; right panel: numbers and median volumes of tumors ($n = 4$ for ENG^+ cells and $n = 3$ for ENG^- cells; Student t test; scale bars, 2 mm). Data are presented as the mean \pm SD. All organ clearance and imaging were performed on day 35. * $P < .05$; n.s., not significant

Culture, Sports, Science and Technology (MEXT) of Japan (17H06326 to K. Miyazono and SE), a KAKENHI Grant-in-Aid for Scientific Research (C) from the Japan Society for the Promotion of Science (JSPS) (19K07684 to SE), and the Princess Takamatsu Cancer Research Fund (to SE). This work was also supported in part by a grant from the Endowed Department (Department of Medical Genomics) from Eisai Co., Ltd.

DISCLOSURE

The authors have no conflict of interest.

ORCID

Jun Nishida  <https://orcid.org/0000-0001-5098-9361>

Shimpei I. Kubota  <https://orcid.org/0000-0003-3188-3988>

Kohei Miyazono  <https://orcid.org/0000-0001-7341-0172>

Shogo Ehata  <https://orcid.org/0000-0002-6740-9391>

REFERENCES

- Capitania U, Bensalah K, Bex A, et al. Epidemiology of renal cell carcinoma. *Eur Urol*. 2019;75:74-84.
- Atkins MB, Tannir NM. Current and emerging therapies for first-line treatment of metastatic clear cell renal cell carcinoma. *Cancer Treat Rev*. 2018;70:127-137.
- Kreso A, Dick J. Evolution of the cancer stem cell model. *Cell Stem Cell*. 2014;14:275-291.
- Battle E, Clevers H. Cancer stem cells revisited. *Nature Med*. 2017;23:1124-1134.
- Kuşoğlu A, Biray Avcı Ç. Cancer stem cells: a brief review of the current status. *Gene*. 2019;681:80-85.
- Khan MI, Czarnecka AM, Helbrecht I, Bartnik E, Lian F, Szczylik C. Current approaches in identification and isolation of human renal cell carcinoma cancer stem cells. *Stem Cell Res Ther*. 2015;6:178.
- Corrò C, Moch H. Biomarker discovery for renal cancer stem cells. *J Pathol Clin Res*. 2018;4:3-18.
- Nishida J, Miyazono K, Ehata S. Decreased TGFB3/betaglycan expression enhances the metastatic abilities of renal cell carcinoma cells through TGF- β -dependent and -independent mechanisms. *Oncogene*. 2018;37:2197-2212.
- Nishida J, Momoi Y, Miyakuni K, et al. Epigenetic remodelling shapes inflammatory renal cancer and neutrophil-dependent metastasis. *Nat Cell Biol*. 2020;22:465-475.
- Taguchi L, Miyakuni K, Morishita Y, et al. c-Ski accelerates renal cancer progression by attenuating transforming growth factor β signaling. *Cancer Sci*. 2019;110:2063-2074.
- Takahashi K, Ehata S, Miyauchi K, Morishita Y, Miyazawa K, Miyazono K. Neurotensin receptor 1 signaling promotes pancreatic cancer progression. *Mol Oncol*. 2021;15:151-166.
- Takahashi K, Ehata S, Koinuma D, et al. Pancreatic tumor microenvironment confers highly malignant properties on pancreatic cancer cells. *Oncogene*. 2018;37:2757-2772.
- Dallas NA, Samuel S, Xia L, et al. Endoglin (CD105): a marker of tumor vasculature and potential target for therapy. *Clin Cancer Res*. 2008;14:1931-1937.
- Zhang YE. Non-smad signaling pathways of the TGF-beta family. *Cold Spring Harb Perspect Biol*. 2017;9:a022129.
- Schoonderwoerd MJA, Goumans MTH, Hawinkels LJAC. Endoglin: beyond the endothelium. *Biomolecules*. 2020;10:289.
- Dorff TB, Longmate JA, Pal SK, et al. Bevacizumab alone or in combination with TRC105 for patients with refractory metastatic renal cell cancer. *Cancer*. 2017;123:4566-4573.
- Choueiri TK, Zakharia Y, Pal S, et al. Clinical results and biomarker analyses of axitinib and TRC105 versus axitinib alone in patients with advanced or metastatic renal cell carcinoma (TRAXAR) [published online ahead of print April 7, 2021]. *Oncologist*. 2021. <https://doi.org/10.1002/onco.13777>
- Saroufim A, Messai Y, Hasmim M, et al. Tumoral CD105 is a novel independent prognostic marker for prognosis in clear-cell renal cell carcinoma. *Br J Cancer*. 2014;110:1778-1784.
- Bussolati B, Bruno S, Grange C, Ferrando U, Camussi G. Identification of a tumor-initiating stem cell population in human renal carcinomas. *FASEB J*. 2008;22:3696-3705.
- Hu J, Guan W, Liu P, et al. Endoglin is essential for the maintenance of self-renewal and chemoresistance in renal cancer stem cells. *Stem Cell Rep*. 2017;9:464-477.
- Kubota SI, Takahashi K, Nishida J, et al. Whole-body profiling of cancer metastasis with single-cell resolution. *Cell Rep*. 2017;20:236-250.
- Takahashi K, Kubota SI, Ehata S, Ueda HR, Miyazono K. Protocol for imaging and analysis of mouse tumor models with CUBIC tissue clearing. *STAR Protoc*. 2020;1:100191.
- Kubota SI, Takahashi K, Mano T, et al. Whole-organ analysis of TGF-beta-mediated remodelling of the tumour microenvironment by tissue clearing. *Commun Biol*. 2021;4:294.
- Scharpfenecker M, van Dinther M, Liu Z, et al. BMP-9 signals via ALK1 and inhibits bFGF-induced endothelial cell proliferation and VEGF-stimulated angiogenesis. *J Cell Sci*. 2007;120:964-972.
- Wiza C, Nascimento EBM, Ouwens DM. Role of PRAS40 in Akt and mTOR signaling in health and disease. *Am J Physiol Endocrinol Metab*. 2012;302:1453-1460.
- Hermida MA, Dinesh Kumar J, Leslie NR. GSK3 and its interactions with the PI3K/AKT/mTOR signalling network. *Adv Biol Regul*. 2017;65:5-15.
- Gallegiante V, Rutigliano M, Sallustio F, et al. CTR2 identifies a population of cancer cells with stem cell-like features in patients with clear cell renal cell carcinoma. *J Urol*. 2014;192:1831-1841.
- van Schaijik B, Davis PF, Wickremesekera AC, Tan ST, Itinteang T. Subcellular localisation of the stem cell markers OCT4, SOX2, NANOG, KLF4 and c-MYC in cancer: a review. *J Clin Pathol*. 2018;71:88-91.
- Khan MI, Czarnecka AM, Lewicki S, et al. Comparative gene expression profiling of primary and metastatic renal cell carcinoma stem cell-like cancer cells. *PLoS One*. 2016;11:e0165718.
- Hu J, Guan W, Yan L, Ye Z, Wu L, Xu H. Cancer stem cell marker endoglin (CD105) induces epithelial mesenchymal transition (EMT)

- but not metastasis in clear cell renal cell carcinoma. *Stem Cells Int.* 2019;2019:9060152-9060159.
31. Fiedorowicz M, Khan MI, Strzemecki D, et al. Renal carcinoma CD105-/CD44- cells display stem-like properties in vitro and form aggressive tumors in vivo. *Sci Rep.* 2020;10:5379.
 32. Lee NY, Golzio C, Gatza CE, Sharma A, Katsanis N, Blobe GC. Endoglin regulates PI3-kinase/Akt trafficking and signaling to alter endothelial capillary stability during angiogenesis. *Mol Biol Cell.* 2012;23:2412-2423.
 33. Pal K, Pletnev AA, Dutta SK, et al. Inhibition of endoglin-GIPC interaction inhibits pancreatic cancer cell growth. *Mol Cancer Ther.* 2014;13:2264-2275.
 34. ten Dijke P, Goumans M-J, Pardali E. Endoglin in angiogenesis and vascular diseases. *Angiogenesis (London).* 2008;11:79-89.

SUPPORTING INFORMATION

Additional supporting information may be found online in the Supporting Information section.

How to cite this article: Momoi Y, Nishida J, Miyakuni K, et al. Heterogenous expression of endoglin marks advanced renal cancer with distinct tumor microenvironment fitness. *Cancer Sci.* 2021;112:3136-3149. <https://doi.org/10.1111/cas.15007>